Proceedings of the 21st ICSMGE, Vienna, Austria, 14 – 19 June 2026. Pistrol, Adam & Schweiger (eds.)
Published by: ÖGG, Austrian Society for Geomechanics, Salzburg, Austria, ISBN 978-3-9503898-4-5
https://doi.org/10.53243/ICSMGE2026-929

Stabilisation of iron mine tailings with high-Ca alkaline cement

Sara Rios, Isabela Caetano, Nelson Mica, António Viana da Fonseca
CONSTRUCT-GEO – University of Porto - Faculty of Engineering, Portugal

Paula Milheiro-Oliveira
CMUP, CONSTRUCT-GEO – University of Porto - Faculty of Engineering, Portugal

Luís Sousa, **Nuno Cristelo**
CQ-VR – University of Trás-os-Montes e Alto Douro - School of Science and Technology, Portugal, ncristel@utad.pt

ABSTRACT: Dry stacking of mine tailings reduces water storage and dam risks, but the mechanical response of the compacted, partially saturated deposits remains a key design uncertainty. This study investigates the stabilisation of iron-ore tailings with a high-Ca alkali-activated binder tailored to deliver the minimum strength needed for cemented berms while preserving granular behaviour. Iron tailings and a Class-F fly ash were used; a NaOH solution, with low lime content, was the activator. Binder proportions were optimised via a response-surface methodology, resulting in fly ash/soil = 0.3, soil/lime = 2.1 and 2.2 m NaOH. XRF/XRD confirmed quartz- and hematite-rich tailings and a quartz–mullite fly ash with a pronounced amorphous hump. Cylindrical specimens were compacted and cured at 40 °C. UCS and CID tests were performed. Total suction was measured to support soil–water retention curve (SWRC) interpretation. Two densities were examined for UCS: low density (≈1.76 g cm^{-3}) and high density (≈1.99 g cm^{-3}). Converting loads to stress using nominal diameters, UCS ranged 0.23–0.32 MPa for the low-density set and 0.98–1.60 MPa for the high-density set, confirming compaction as a significant strength contributor and meeting the ~1 MPa target for berm design. The CD triaxial test showed a peak deviator stress at $\varepsilon_a \approx 2.3\%$, followed by softening; volumetric strain was contractive at small strains, transitioning to dilation beyond ~2.3%, consistent with fabric rearrangement and interlocking typical of lightly cemented granular soils. The SWRC for the (unstabilised) tailings indicated air-entry at 8–12 kPa, a sharp desaturation from $\theta w \approx 38\%$ to 17% between 5–12 kPa, and a near-residual regime for $\psi \gtrsim 100$ kPa; stabilisation is expected to shift the curve upward/right due to pore refinement. Overall, the high-Ca AAB provides the required strength at modest dosage, preserves granular behaviour, and offers a lower-carbon route for constructing stabilising berms in dry-stacked tailings.

KEYWORDS: alkali-activated binders, cemented materials, soil-water characteristic curve, unconfined compression strength.

1 INTRODUCTION

The exploration of mineral resources is essential for modern society, but it generates large quantities of fine-grained residues known as tailings during the ore extraction and processing. Traditionally, tailings are disposed of as hydraulic fills in dams. However, the failure of these structures often results in catastrophic mudflows, with severe environmental, social, and economic consequences, including loss of life and disruptions in raw material supply. The increasing number of tailings dam failures highlights the urgent need for safer and more sustainable disposal strategies.

Dry stacking has emerged as an alternative to conventional tailings dams. In this method, tailings are filtered and compacted to form stable embankments with reduced water content. Despite the term "dry," these tailings still retain some moisture, with their degree of saturation depending on factors such as filtration efficiency, grain size, transport, and climate conditions (Davies, 2011). As a result, their strength can vary significantly due to changes in compaction, drainage, loading conditions, and excess pore pressures. Furthermore, these structures face height limitations due to high overburden stresses.

Even with drainage systems, filtered dry stacks may become saturated after heavy rainfall, particularly under inefficient drainage conditions. Poorly compacted tailings can exhibit contractive behaviour under medium to high confining pressures, leading to liquefaction risks. Past failures of dry stacks during periods of intense rainfall indicate that reinforcement solutions are necessary, especially under the evolving challenges of climate change.

One reinforcement strategy involves building cemented berms or structural zones using filtered tailings (Caetano et al., 2023; Viana da Fonseca et al., 2024, Ribeiro et al., 2025). While Portland cement (PC) has been widely studied for stabilising iron tailings (Consoli et al., 2018; 2022; Jahanshahi and Ghanizadeh, 2024), its production is energy-intensive and has a high carbon footprint. To address this limitation, this study explores the use of high-Ca alkaline cement, an alternative binder produced by activating industrial by-products (e.g., coal fly ash) with alkaline solutions. These binders, also known as alkaline activated binders (AABs), can significantly reduce carbon emissions while promoting circular economy principles (Cristelo et al., 2015).

Although there is a growing body of research on the stabilisation of mine tailings using AABs (Pereira dos Santos et al., 2022; Manaviparast et al., 2024), their unsaturated behaviour and mechanical response under field-like conditions remain poorly understood. This paper investigates the soil–water retention behaviour and mechanical performance of iron mine tailings stabilised with a high-Ca alkaline cement, with particular focus on the implications for the design of stable, low-carbon dry stacks.

2 MATERIALS AND METHODS

2.1 *Iron ore tailings, precursor and activator*

The iron ore tailings used in this work is from Minas Gerais (Brazil). As is usually the case, the unit weight of the particles (γ_s=29.5kN/m3) is quite high when compared to those usually found in natural soils, due to the higher iron content. The tailings are classified as non-plastic. Its grain size distribution curve can be seen in Figure 1. The chemical composition of the tailings, determined by XRF and presented in Table 1, reveals that 99% of the content is silica and iron oxide, with the silica representing the major share. Accordingly, the X-Ray

diffraction analysis, presented in Figure 2, reveals the presence of silica- and iron-based phases, namely quartz and hematite.

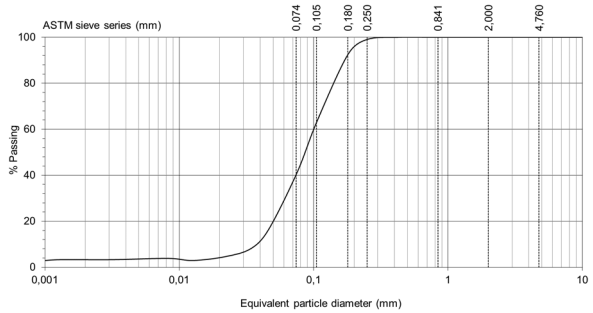

Figure 1: Iron tailing grain size distribution curve

Table 1: Elemental composition of the materials (%)

Element	Fly ash	Tailings
SiO2	59.69	76.64
Al2O3	20.11	0.28
Fe2O3	7.15	22.4
MnO	0.07	0.07
CaO	1.28	0.16
MgO	1.72	<0.20
Na2O	1.22	<0.20
K2O	2.16	<0.05
TiO2	0.92	<0.04
P2O5	0.05	<0.04
LOI	5.36	0.24

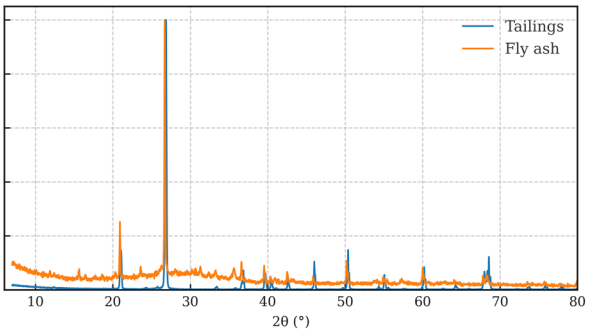

Figure 2: X-Ray diffractograms of the tailings and fly ash

The precursor used in this work was a low calcium fly ash, classified as class F according to the ASTM standard C 618. Sodium hydroxide was used as activator, while lime was added to specific formulations, to increase the calcium content of the paste. The chemical composition of the fly ash is also included in Table 1, showing a typical Class-F coal ash, composed by more than 85% of silica, alumina and iron oxide. Its X-Ray diffractogram (Figure 2) shows mostly peaks associated with quartz and mullite, the main mineralogical phases, and a clear amorphous content, indicated by the hump approximately between the 15-40 (º2θ) range.

2.2 *Binder optimization*

The binder was optimized by applying a statistical methodology based on the response surface method (RSM) to predict the maximum unconfined compression strength of the stabilized tailings resulting from different mixtures. The Design of Experiments underneath the RSM was used to minimize the number of required experiments while providing an efficient tool for data interpretation. From this work, a mixture was selected, which provided the ideal strength while minimizing the AAB components. This mixture has a fly ash/soil ratio of 0.3, a soil/lime ratio of 2.1 and a 2.2 molal NaOH concentration. It should be noted that this optimization process is crucial while developing stabilizing cements for the mining industry, as the target UCS should not be the maximum value possible, but, instead, just the sufficient to allow structural integrity and stability, without compromising the normal mechanical behaviour of granular materials – it is important that the stabilized tailings still behave like a granular material, since the transformation in a monolithic cemented block would not only be unnecessary, from a structural point of view, but it would be financially and environmentally more expensive.

2.3 *Specimen preparation and testing*

Cylindrical specimens were prepared for the uniaxial and triaxial tests (Figure 3), with nominal diameters of 35mm and 70mm, respectively, and nominal heights of 70mm and 140mm. Firstly, all dry components - tailings and fly ash - were mixed. After that, the alkaline activator solution was added. The UCS specimens were moulded in three compacted layers, while triaxial specimens, given their superior height, were fabricated using five compacted layers. The procedure followed the contents of ASTM D1632-17, where each layer has the same amount of soil mixture. After demoulded, all specimens were cured at 40ºC, in a climatic chamber.

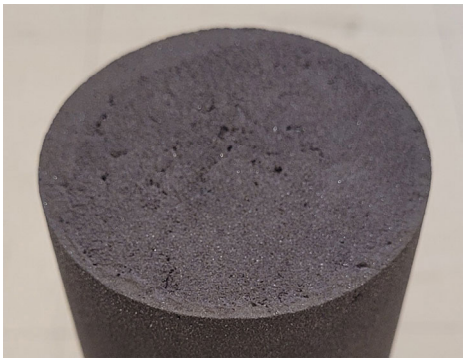

Figure 3: General aspect of a stabilized specimen (triaxial)

The uniaxial strength tests were performed on a bench load frame, under a constant displacement rate of 0.05 mm/min and using a 5 kN load cell.

Consolidated–drained (CD) triaxial tests were performed in accordance with BS 1377-8. Specimens were saturated by back-pressure (up to 500 kPa) until Skempton's B-value reached 0.96, then isotropically consolidated to an effective confining stress σ'_3 = 100 kPa (until ~95% primary consolidation was achieved, based on the volumetric response). Axial loading was applied at a constant displacement rate of 0.006 mm/min, and tests were terminated at 20% axial strain. Local Hall-effect transducers measured axial and radial strains directly on the specimen (Figure 4), from which volumetric strain ($\varepsilon v = \varepsilon a + 2\varepsilon r$) was computed. Pore water pressures were monitored with pressure transducers throughout the tests, to verify full excess pore pressure dissipation during consolidation and drained shearing.

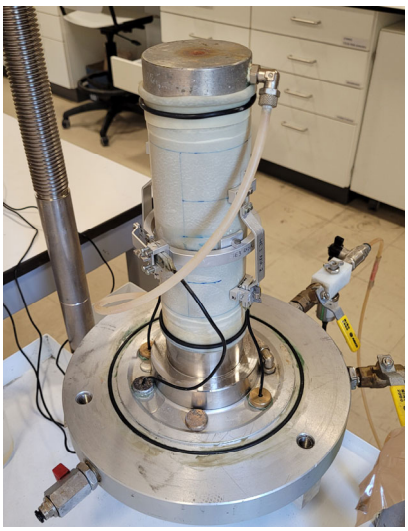

Figure 4: Setup of the triaxial test, showing Hall-effect displacement transducers

2.4 *Water retention curves*

Total suction was measured with a WP4C dewpoint potentiometer (METER Group). Small sub-samples of the tailings (or cemented tailings) were gently compacted inside appropriate flat capsules (Figure 5), which were then placed into the instrument's sample trey, avoiding smearing or contact with the cup rim. The WP4C determines water potential by determining the dewpoint of a chilled mirror: the vapour above the sample is cooled until condensation forms, from which the device computes the sample's water potential (ψ, in MPa). Reported ψ values were converted to suction and used to construct the soil-water retention curves. Because the system measures total suction, both matric and osmotic contributions are captured – which is relevant for the alkaline, ion-rich pore solutions produced inside these cemented specimens. Measurements were recorded once the instrument's stability criterion indicated equilibrium, and sample cups/chamber were cleaned between runs to prevent cross-contamination.

Figure 5: General aspect of a WP4C compacted specimen

3 MECHANICAL PERFORMANCE

The mechanical performance was first assessed using uniaxial compressive strength tests, mostly to confirm that the UCS of this particular formulation was approximately 1 MPa – the optimum axial reference strength, previously defined as necessary to maintain a granular material behaviour. UCS results can be seen in Figure 6, for two sets of specimens with the exact same formulation, but different densities, namely 1.76 g/cm^3 and 1.99 g/cm^3. The higher density specimens (UCS 04 to UCS 06) produced a significantly better response, highlighting the importance of an effective compaction of the stabilized materials and, also, confirming that, regardless of the cement addition, granular-type behaviour was maintained. Based on these results, the higher density was assumed for the triaxial test specimen.

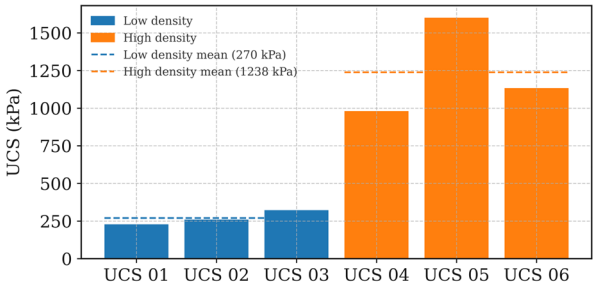

Figure 6: Compressive strength test results

Figure 7 presents the mechanical and volumetric responses during shearing. The upper plot shows the deviator stress q versus axial strain ε_a, while the lower plot shows the volumetric strain ε_v, also versus the ε_a. Volumetric strain was computed from the Hall-effect transducers, while these were still functioning correctly, and, subsequently, from the piston-type volume change apparatus. The figure highlights an initial pronounced peak in deviator stress (at a strain of approximately 2.3%) followed by slight stiffness, until the 8.0% strain, and progressive softening afterwards.

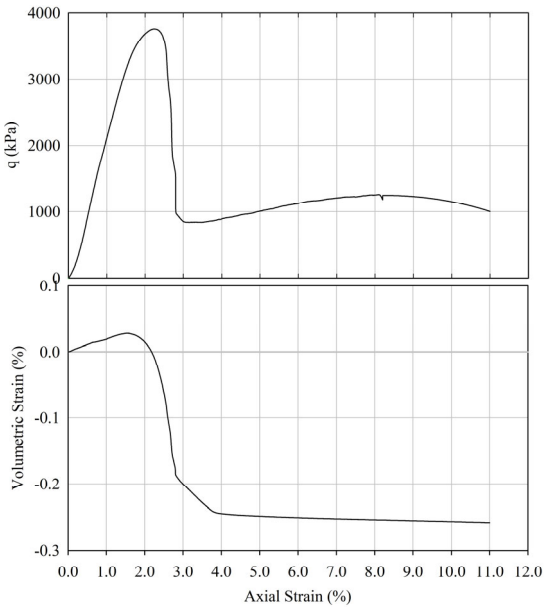

Figure 7: Compressive strength test results

Meanwhile, the volume strain shows an immediate contraction, indicating that the soil fabric is collapsing, and contacts rearrange more efficiently, so an increment of axial strain produces a small decrease in volume. The rate of contraction $d\varepsilon_v/d\varepsilon_a$ peaks before or near the stress peak then diminishes as interlocking saturates. After approximately 2.3% axial strain, the curve crosses over and dilation begins. This rapid and significant dilation, after the early segment of the shearing, is the result of a contact rearrangement and increased particle interlocking, causing an increase in volume as the fabric starts to gradually mobilize strength. As the axial strain accumulates, the volume change starts to stabilise, resulting in less void space left available. Consequently, the $d\varepsilon_v/d\varepsilon_a$ is reduced and the

curve flattens. The post-8.2% segment remains dilative but trends toward a lower, near-steady rate.

Viewed together, the two curves show coupled mechanical-volumetric evolution. Deviator stress rises to a peak and then softens; while over the same axial strain range the specimen slightly contracts, at first, and then rapidly dilates at a faster pace. Most of the volumetric change is built before or around the start of the plastic behaviour, when fabric rearrangement is most active. Beyond the peak, the q/ε_a curve abruptly decreases, consistent with damage localization and reduced incremental strength, while the corresponding $\varepsilon_v/\varepsilon_a$ slope reflects the fabric adapting to the new stress state.

This behaviour is typical of cemented soils with peak stress followed by strain softening and high initial stiffness (Rios et al., 2014, 2016).

4 SOIL WATER CHARACTERISTIC CURVE

Figure 8 shows the soil-water retention curve for the original mine tailings, compacted at the same high density (1.99 g/cm^3) that was used for the triaxial test specimens. It represents the suction ψ (log scale) versus the gravimetric water content θ_w. The data indicates a strong desaturation at low suction, as the θ_w falls from approximately 38% to 17%, between 5 and 12 kPa, suggesting an air-entry value in the 8 to 12 kPa range. A steep transition persists to approximately 50 kPa, after which the θ_w tends toward a residual regime. For $\psi \gtrsim 100$ kPa, the water content is essentially constant and near zero, consistent with drainage of macropores and progressive emptying of finer pores. After cement stabilization, the retention curve should typically shift upwards and to the right, showing higher air-entry suction and a higher residual content due to pore refinement by hydration products.

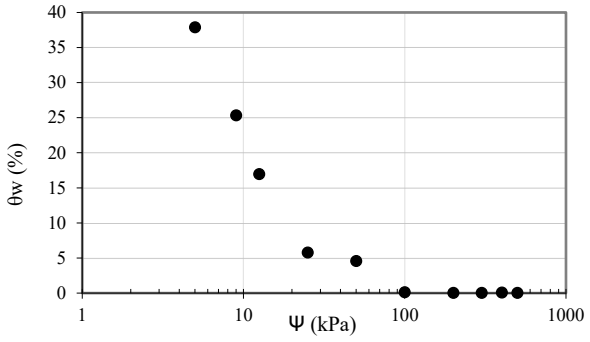

Figure 8: Soil water retention curve of the original (unstabilised) tailings

5 CONCLUSIONS

A high-Ca alkali-activated binder, optimised by response-surface methods, effectively stabilises iron tailings while meeting a practical target strength (~1 MPa) for cemented berms. Strength is governed primarily by density: UCS increased from ~0.27 MPa (low density) to ~1.24 MPa (high density). CD triaxial results exhibit a peak at ~2.3% axial strain with contractive–dilative transition, confirming that the mixture preserves granular-type behaviour rather than forming a brittle monolith. The tailings SWRC shows air-entry at 8–12 kPa and rapid desaturation at low suction, informing suction-dependent design. The proposed AAB approach reduces Portland-cement demand and supports safer, lower-carbon dry-stack tailings infrastructure; future work will address unsaturated triaxial response and durability/leaching.

6 ACKNOWLEDGEMENTS

This work was financially supported by national funds through the FCT/MCTES (PIDDAC), namely the CONSTRUCT - Instituto de I&D em Estruturas e Construções (UIDB/04708), the research project INPROVE-2022.02638.PTDC (https://doi.org/10.54499/2022.02638.PTDC), and by scholarship 2022.13858.BD to the second author. Also to mention the partial support from CMUP, member of LASL, which is financed by national funds through FCT under the project with reference UIBD/00144/2020.

7 REFERENCES

ASTM D1632-17, Standard Practice for Making and Curing Soil-Cement Compression and Flexure Test Specimens in the Laboratory, ASTM International, 2017

Caetano, I., Rios, S., Da Fonseca, A. and Delgado, B., 2023. Stabilization of iron tailings with alkali activated binders. 1st International Conference on Geotechnics of Tailings and Mine Waste. Ouro Preto, Minas Gerais, Brasil.

Consoli, N.C., da Silva, A.P., Nierwinski, H.P. and Sosnoski, J., 2018. Durability, strength, and stiffness of compacted gold tailings – cement mixes. Canadian Geotechnical Journal, 55(4), pp.486–494. https://doi.org/10.1139/cgj-2016-0391.

Consoli, N.C., Vogt, J.C., Silva, J.P.S., Chaves, H.M., Scheuermann Filho, H.C., Moreira, E.B. and Lotero, A., 2022. Behaviour of Compacted Filtered Iron Ore Tailings–Portland Cement Blends: New Brazilian Trend for Tailings Disposal by Stacking. Applied Sciences, 12(2), p.836. https://doi.org/10.3390/app12020836.

Cristelo, N., Miranda, T., Oliveira, D., Rosa, I., Soares, E., Coelho, P. and Fernandes, L., 2015. Assessing the production of jet mix columns using alkali activated waste based on mechanical and financial performance and CO2 (eq) emissions. Journal of Cleaner Production, 112, 447–460. https://doi.org/10.1016/j.jclepro.2015.04.102.

Davies, M., 2011. Filtered dry stacked tailings : the fundamentals. In: Proceedings Tailings and Mine Waste 2011. [online] Proceedings Tailings and Mine Waste 2011. Vancouver, BC, Canadá. https://doi.org/10.14288/1.0107683.

E 264, E.L., 1972. E 264-1972 - Solo- Cimento Ensaio de Compressão. Portugal.

Jahanshahi, F.S. and Ghanizadeh, A.R., 2024. Compressive strength, durability, and resilient modulus of cement-treated magnetite and hematite iron ore tailings as pavement material. Construction and Building Materials, 447, p.138076. https://doi.org/10.1016/j.conbuildmat.2024.138076.

Manaviparast, H.R., Miranda, T., Pereira, E. and Cristelo, N., 2024. A Comprehensive Review on Mine Tailings as a Raw Material in the Alkali Activation Process. Applied Sciences, 14(12), p.5127. https://doi.org/10.3390/app14125127.

Pereira dos Santos, C., Bruschi, G.J., Mattos, J.R.G. and Consoli, N.C., 2022. Stabilization of gold mining tailings with alkali-activated carbide lime and sugarcane bagasse ash. Transportation Geotechnics, 32, p.100704. https://doi.org/10.1016/j.trgeo.2021.100704.

Ribeiro, L., Rios, S., Arroyo, M. and Manica, M. (2025). A parametric study on the stability of tailings storage facilities with cemented berms. Soils and Rocks, (accepted for publication)

Rios, S., Viana da Fonseca, A. and Baudet, B. (2014). On the shearing behaviour of an artificially cemented soil. Acta Geotechnica, 9(2), 215-226, doi: 10.1007/s11440-013-0242-7

Rios, S., Cristelo, C., Viana da Fonseca, A., Ferreira, C. (2016). Structural Performance of Alkali Activated Soil-Ash versus Soil-Cement. Journal of Materials in Civil Engineering, 28(2), 1-11, DOI: 10.1061/(ASCE)MT.1943-5533.0001398

Viana da Fonseca, A., Caetano, I., Meneses, B. and Rios, S., 2024. Tailing Storage Facilities with Cemented Berms for Sustainable Production of Raw Materials. In: P. Duc Long and N.T. Dung, eds. Proc. 5th International Conference on Geotechnics for Sustainable Infrastructure Development. Singapore: Springer Nature. 1099–1111. https://doi.org/10.1007/978-981-99-9722-0_72.